Description of the EPOXI MRI Photometry of Comet 103P/Hartley 2

Version 2: August 2016

Dennis Bodewits, Tony Farnham, Mike A'Hearn
University of Maryland

Version 1: December 2012

Stephanie McLaughlin, Jade Williams, Dennis Bodewits
University of Maryland
Jian-Yang Li, Planetary Science Institute

1 Overview

We perform photometric measurements of comet 103P/Hartley 2 using images taken through the CLEAR1 (broadband, 200-1100 nm), CN (387 nm), OH (309 nm), C_2 (514 nm), and two continuum filters (Ultraviolet at 345 nm and Green at 526 nm) of the Medium Resolution Instrument (MRI) on board the Deep Impact flyby spacecraft from 1 October to 26 November 2010 during the EPOXI mission. Our analysis includes over 30,000 MRI science images where the nucleus was not resolved. We apply two different methods for our analysis: simple aperture photometry using circular apertures and azimuthally-averaged photometry using concentric annuli to remove stars. The resulting photometry and computed errors from each method are provided as separate ASCII tables along with PDS labels describing the layouts and columns. A comparison with Version 1 of this dataset (Laughlin et al. 2012) is given in Sec. 6.

2 Instrument

The Medium Resolution Instrument consists of a Cassegrain telescope with a 12 cm aperture and a 2.1 m focal length and a CCD. The detector is a 1024x1024 split-frame, frame-transfer CCD with 21-micron-square pixels. The electronics allow readout of centered sub-frames in multiples of 2: 64x64, 128x128, and so on. The net pixel scale is 10 microradians/pixel (2.06 arcseconds/pixel). MRI images were never binned at Hartley 2. The full-width half-max (FWHM) of the point spread function is approximately 1.6 pixels (Klaasen et al., 2013). The MRI has nine filters. Some were only used during close-encounter, and our sample only includes these six. More detailed information regarding these filters can be found in Klaasen, et al., 2012, and Hampton, et al., 2005.

The two central rows of the CCDs in each camera are 1/6 of a pixel smaller vertically than a normal row (vertical in the standard image display used by the team, see Sec 3.1.1; Klaasen, et al., 2012; Klaasen, et al., 2008; Hampton et al., 2005). However, the pipeline reconstructs raw and calibrated images with uniform row spacing, which introduces a 1/3rd-pixel, horizontal extension at the center of the array. Therefore, the actual angular separation of two features on either side of the horizontal midpoint line but outside of the two central rows is 1/3rd -pixel less than the separation measured in a reconstructed image. As for all

Table 1 – MRI Filter characteristics

Filter #	Filter Name	Center (nm)	FWHM (nm)	Eff. Wavelength (nm)	Comments
1	CLEAR1	650	>700	626.1	Not band limited
2	C2	514	11.8	515.3	For C_2 coma studies
3	GREEN_CONT	526	5.6	526.0	For dust in coma
7	CN	387	6.2	388.8	For CN coma studies
8	VIOLET_CONT	345	6.8	345.5	For dust in coma
9	OH	309	6.2	309.5	For OH coma studies

geometric distortions, the correction for this distortion requires resampling of the image and an attendant loss in spatial resolution. The DI calibration pipeline does not perform this geometric correction, in order to preserve the best spatial resolution outside of the two central rows. However, using the flat-field division, the pipeline does correct for the 1/6 decrease of signal due to the smaller collecting area in the two narrower central rows, so that the pixels in those two rows have the correct scene radiance in the calibrated images. This preserves the surface brightness measurement everywhere in the geometrically distorted image. Point source or disk integrated photometric measurements using aperture photometry that includes these two central rows will be slightly distorted unless special adjustments are made. For example, Appendix A of Belton, et al. (2012), describes the method of subtracting $1/6^{th}$-pixel worth of signal from the two central rows and adjusting for the geometric distortion in calibrated MRI images of comet 9P/Tempel 1 before performing photometry. We apply a different approach for Hartley 2 photometry, which is described below. We refer to this process of recovering the original scene radiance as the 'gap correction'.

3 Photometry Process

Our photometry process consists of the following steps, which we describe below:

1. Start with reversibly calibrated images and a list of comet centroid coordinates as the inputs
2. Assign a quality flag to each image
3. Remove cosmic rays
4. Apply the gap correction
5. Perform simple aperture photometry
6. Perform azimuthally averaged photometry
7. Compute photometric uncertainties

3.1 Input Data

3.1.1 Reversibly Calibrated Images

We use the reversibly calibrated (RADREV) MRI science images of Hartley 2 archived in the NASA Planetary Data System (McLaughlin, et al., 2012) as input to this photometric analysis. We restrict the analysis to "good" images taken through the CLEAR1, CN, C2, OH, Green Continuum, and Ultraviolet Continuum filters where the nucleus was not resolved. 'Good' images are defined in section 3.2.

The RADREV images have had the standard EPOXI pipeline corrections applied to them: bias and dark frame subtraction, flat-field corrections, horizontal stripe removal (only a minority of CLEAR1 images), etc. (Klaasen, et al., 2008; 2012). They have not, however, been processed to remove artifacts such as cosmic rays and bad pixels.

We define the following image display orientation and pixel coordinate notation for our analysis. All RADREV images are displayed using the FITS convention where lines increase up and samples increase to the right. Our pixel coordinate notation is zero-based with the first coordinate (0,0) located at the center of the pixel in the lower left corner of the display window, and the pixel coordinate of the center of the full-frame, 1024x1024 image is (511.5, 511.5). Figure 1 (Klaasen, et al., 2008) shows a full-frame MRI image from the Deep Impact prime mission displayed with this convention. We refer to quadrants A and B as the top or upper half of the image and quadrants C and D as the bottom or lower half.

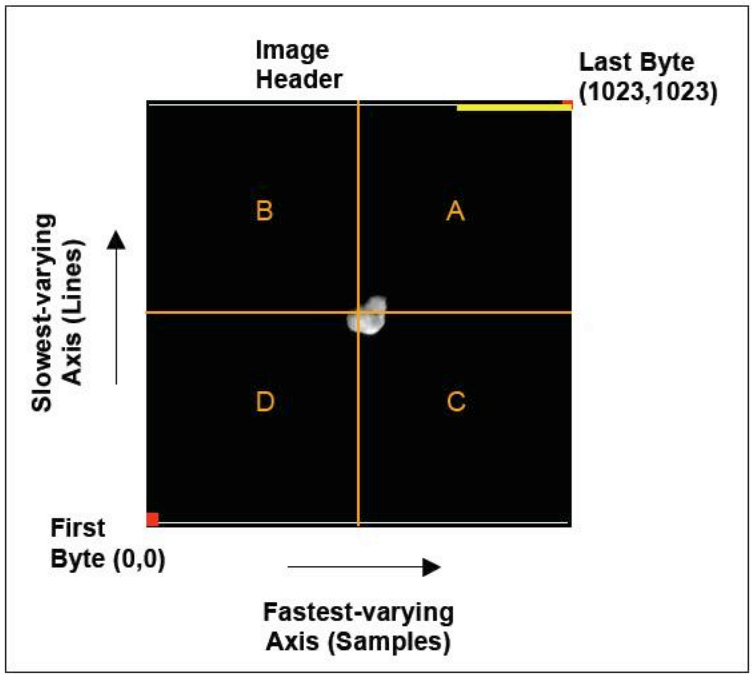

Figure 1. MRI image orientation and display conventions (Klaasen et al. 2008).

Although Figure 1 shows a full 1024x1024 MRI frame, all images we use in our analysis were taken with smaller sub-frame modes: 512x512, 256x256, and 128x128 pixels centered on the middle of the CCD. All MRI data at Hartley 2 were unbinned.

As previously noted, the calibration pipeline corrects for the 1/6th signal decrease in each of the two narrower central rows by the flat-field division so that the pixels in those two rows have the correct scene radiance in the calibrated RADREV images.

3.1.2 Centroid Coordinates

The second input to our photometric process in a list of centroid coordinates for the RADREV images. The photo-center of the coma was typically computed using the CNTRD routine found in the IDL Astronomy User's Library maintained by NASA Goddard Space Flight Center (GSFC). These centers are good to approximately 1/3 pixel, given the under-sampled

point spread function (PSF). For images where the CNTRD routine did not converge because of trailing or other distortion, the centroid was selected manually to represent the apparent center of the coma. These centers are good to about a pixel, and can be identified by the fact that they are given to the nearest integer. The centroid coordinates, which are captured in the resulting photometry and error tables, are zero based with (0,0) assigned to center of the pixel in the lower-left corner of an image (Fig. 1).

3.2 Image Quality Flags

Before performing photometry, we manually inspect each RADREV image that has centroid coordinates and assign an image quality flag:

0: Good quality image
1: Star located within a 9-pixel radius of the centroid, possibly affecting small-aperture photometry
2: Cosmic ray located within a 9-pixel radius of the centroid, affecting small-aperture photometry
3: IR context image
4: Saturated image, or nucleus resolved during close approach
5: Smeared image (due to incorrect spacecraft slew rate)
6: Corrupt image

We recommend using only measurements from images with a quality flag of 0, 1, or 2. We call these images 'good'.

3.3 Cosmic Ray Removal

All MRI images are affected by cosmic rays, with their number increasing with exposure time. To exclude cosmic rays from our photometric measurements, we process all "good" RADREV images through an IDL routine called IMGCLEAN (written by Erik Deutsch/STSCI) that identifies very bright pixels and replaces those pixels with values derived by interpolation of the surrounding, well-behaved pixels. (IMGCLEAN performs a PSF match to avoid confusing cosmic rays with stars.)

3.4 Gap Correction

Disk-integrated photometric measurements using aperture photometry that include the central two rows of RADREV images will be slightly distorted unless special adjustments are made. For our analysis, we correct for the central gap by resampling both halves of a RADREV image with linear interpolation to effectively push them inward, such that the central two rows are reduced by a total width of 1/3 pixel. The procedure we implement starts the correction from the two central rows by decreasing their radiance by 1/6 to undo the 'scene radiance correction' of the flat field division performed by the calibration pipeline. Then our procedure moves 1/6 of the radiances from the next adjacent rows outward for all rows. The first and last rows of the gap-corrected images contain lower fluxes than the real radiances and should not be used. The resulting images have thus been corrected for the gap in both a photometric and a geometric sense. We apply this correction to all images before photometric measurements. The centroid of the comet is adjusted by 1/6 pixel inward if outside of the two central rows or recomputed in the corrected images using the procedure described in Section 3.1.2 if inside the two central rows. In theory, this correction does not change the measured

flux when the aperture size is smaller than the vertical distance between the comet centroid and the CCD center row. But because linear interpolation is involved with the non-linear brightness distribution of the coma, especially at small cometocentric distances, the flux for small apertures that do not cross the two central rows is still slightly affected by the correction. See Section 3.7 for more details on the photometric uncertainties. We find this method of gap correction significantly improves the photometry, most notably for measurements using the smallest apertures.

3.5 Small Aperture Photometry

We use the APER routine found in the GSFC's IDL Astronomy User's Library to calculate photometry on the cleaned, calibrated RADREV images. No background was subtracted ('Skylevel=0'), and the program was used to compute the photometric errors of Poisson photon counting noise using a CCD gain of 28.5 electrons/DN (Klaasen et al., 2008). We use the following aperture radii, in pixels: 3, 4, 5, 6, 7, 8, 9, 10, 12, 14, 16, 18, 20. We do not recommend using apertures with a radius smaller than 3 pixels (PSF) for photometry. We do not scale the resulting photometry or errors for phase angle or distance effects (i.e., the range between the spacecraft and the comet and the heliocentric distance of the comet).

We note that comet Hartley 2 was in a dense star-field as observed from the spacecraft during both approach and departure. The presence of stars severely interferes with photometric measurements with large aperture sizes, typically those larger than 20 pixels in radius. We did not perform any rejection of stars in the simple aperture photometry measurements, but only flagged those images with stars located within 9 pixels from the comet. Therefore, users should exercise extra caution when using the aperture photometry for aperture radii larger than 9 pixels (outside the region where we checked for stars and flagged the images). Because of the discrepancies introduced by the stars in the larger apertures, we recommend the photometric measurements obtained using the technique described in Section 3.6 when results from aperture radii larger than 10 pixels are desired.

3.6 Azimuthally-Averaged Photometry

In order to minimize the contamination from background stars, we developed the so-called 'azimuthally-averaged photometry' procedure, which measures the integrated flux through the mean radial profile of the comet where stars are filtered out using an outlier-resistant determination of the mean. Specifically, we re-project an image into polar projection centered at the comet centroid using the IDL 'cartop.pro' routine[1] (George H. Fisher UCB/SSL), with 1-pixel increments along the radial direction and 1-degree increments along the azimuthal direction. Then we take a 'resistant mean' along the azimuthal direction with a pre-set rejection threshold ('Resistant_mean.pro' is part of GSFC's IDL Astronomy User's Library). This resistant-mean step rejects all bright pixels that belong to stars that are brighter than the threshold from the mean of the cometary coma. The mean represents an azimuthal average of the coma at each increment of radial distance from the photo-center. The result of this step is an average radial surface brightness profile of the coma, with minimal influence from the stars in the field. These surface brightness profiles are part of this archive. The total flux F within a

[1] http://solarmuri.ssl.berkeley.edu/~fisher/public/software/idl/polar-cartesian/

certain aperture ρ is integrated along the average radial surface brightness profile *S(r)* from the center to the aperture radius:

$$F(\rho) = 2\pi \int_0^{\rho} r * S(r)\, dr$$

The star rejection threshold for the resistant mean is set to be 3-sigma except for images taken through CLEAR1 and Green Continuum filters, for which a 3.5-sigma threshold is used. The reason for slightly higher threshold for those two filters is that the dust coma as observed through CLEAR1 and Green Continuum filters appears to have substantial azimuthal variations. A 3-sigma threshold has the potential to reject a small fraction of the coma in the azimuthal directions where coma is the brightest. The coma of Hartley 2 shows obvious azimuthal variations; the results of this method account for those variations. The gas comae as observed through the CN, OH, and C_2 filters appear to be almost azimuthally symmetric.

The resistant mean step requires a sufficient number of pixels within the annulus considered in order to reliably reject bright pixels due to stars. Therefore, this procedure is more reliable for photometric measurements at relatively large aperture sizes. For this reason, as a general guideline, we recommend researchers to use the aperture photometry described in Section 3.5 for aperture sizes smaller than 10-pixel radius, and the photometry results described in this section for larger aperture sizes. Occasionally, a bright star can be within just a few pixels from the center, rendering the calculation of resistant mean unreliable due to the small fraction of pixels in the coma at small radial distances. We flag all images with stars located within 9-pixels from the comet. Thus, the two techniques we have adopted provide complementary results, where the strengths of one offset the deficiencies of the other, allowing photometric measurements to cover apertures from 3 pixels to hundreds of pixels.

Our photometric methods do not include a background subtraction, which includes the sky background as well as bias residuals*,* which includes the sky background as well as bias residuals (1 – 3 DN, Klaasen et al. 2013). We assessed background values for the CLEAR1 and CN filters by looking at the brightness profiles of images with the largest observed radial coverage of about 145,000 km, and evaluating longer exposures taken in the full-frame CCD mode of 1024x1024 pixels. For CLEAR1 images we find that the background varies among images but that it also varies between the quadrants of the CCD. From the edge of the chip, we find that the background surface brightness is of the order of 1 – 2 x 10^{-6} W/m^2/μm/sr and for CN images 1 – 2x 10^{-5} W/m^2/μm/sr. These numbers are consistent with the 1 DN detection limit for typical exposure times (summarized in Table 2). We did not empirically determine background levels for C_2, OH, GC, and UC images because there are only small-frame exposures in these filters when the spacecraft was close to the comet, i.e. the coma fills the entire chip.

Table 2 – 1 DN detection limits for typical exposure times

Filter	**Exposure time (s)**	**1 DN Surface Brightness (W/m2/um/sr)**
CLEAR1	20 – 60	5.9E-7 – 1.8E-6
GC (526)	400	9.2E-6
C2 (514)	400	4.5E-6
CN (387)	400	2.3E-5
VC (345)	400	2.6E-5
OH (309)	400	4.5E-5

Assuming background levels of 10^{-5} W/m^2/μm/sr for CN and 10^{-6} W/m^2/μm/sr for CLEAR1) in the apertures the background may contribute up to 10% of the signal for the largest apertures in the CN and CLEAR1 filter.

3.7 Photometric Uncertainties

The sources of photometric uncertainties include absolute photometric calibration error, the stochastic error, read noise, the error introduced by the 1/3-pixel gap correction, and other errors introduced during the processing for radial profile photometry. They have different characteristics and dominate over ranges of aperture sizes and images. We discuss them one by one below.

The **absolute calibration** error given for the MRI instrument is 20% for UV filters (OH, CN, UC) and 10% for all other filters (Klaasen et al., 2012; Klaasen et al., 2008). This calibration uncertainty is systematic and is the same for all photometric data points. Since the photometric calibration of MRI is stable during the encounter (Klaasen et al., 2012), this uncertainty affects all photometric data points by the same amount. It does not affect point-to-point variations.

The **rejection of cosmic rays** introduces uncertainty in the pixels affected by cosmic rays. The number of affected pixels is usually <1% of total pixels within the aperture, and the associated uncertainty is therefore much less than 1%, and negligible. We did not quantify this uncertainty in our analysis.

The **read noise** of the MRI's CCD is 1 DN (Klaasen et al. 2008). The contribution of the read noise to the surface brightness is the variance of the read noise, which is 1 DN. The read noise N_{RN} in an aperture with radius ρ in units of electrons is:

$$\mathrm{N}_{RN}(\rho) = \sqrt{gain * RN * n_{p\,ix}} = \sqrt{28.5 * 1^2 * \pi\rho^2}$$

Dark current of the CCD is estimated to be $2\text{x}10^{-4}$ DN/s/pixel at typical operating temperatures of -100 C. Typical exposure times for the CLEAR1 filter are 60 s, and 400 s for the CN filter, resulting in 0.01 – 0.1 DN/pixel. The dark current noise N_{DC} in an aperture with radius ρ in units of electrons is:

$$\mathrm{N}_{DC}(\rho) = \sqrt{gain * D * n_{pix} * t_{exp}} = \sqrt{28.5 * 2 * 10^{-4} * \pi\rho^2 * t_{exp}}$$

The **photon counting noise of the surface brightness profiles** follows Poisson statistics as the square root of total electrons accumulated in a pixel on the CCD. We calculated the photon counting noise N_{PC} in the flux with an MRI gain setting as 28.5 (Klaasen, et al., 2008). With increasing distance to the nucleus, counts decrease, and the number of stars and cosmic rays within the aperture increases. Note that cometary comae tend to be fairly smooth, so we expect that interpolating over these features is not likely to be a dramatic change to the values that would have been measured in their absence (barring a star or CR right at the nucleus). To quantify this in the surface brightness profiles, we use the 1-σ standard deviation of the surface brightness distribution within the annulus with radius *r*. For CLEAR1 images, the photon counting noise within a 3-pixel aperture is usually 1% for early approach images (E-60d to E-40d) with long exposures (60 s exposure time), and 0.5% for short exposures (20 s). Within E±40d, the uncertainties are typically <0.3% for long exposure images and <0.5% for short exposures. For CN images, the photon counting noise is typically ~1% for 3-pixel

aperture photometry, and <0.3% for apertures of 20 pixels in radius. The uncertainties for OH photometry are similar to those for CN photometry.

The **correction for the 1/3-pixel gap** introduces uncertainties from the interpolation between pixels and the consequent loss of spatial resolution. We designated this uncertainty as the difference of fluxes between corrected images and uncorrected images. As discussed earlier, for small apertures that do not cross the two central rows, the uncertainty calculated with this method is not exactly zero, but have some low absolute uncertainty values compared to larger apertures that cross the central rows. It is not included in our error calculation.

Summarizing, here are the relations used the calculate relative uncertainties in the photometric dataset:

1. Flux in small apertures: the noise (in units of electrons) in the flux in an aperture with radius ρ is calculated by the quadratic addition of the read noise N_{RN} and the photon counting noise N_{PC} calculated from the flux F (in DN):

$$N(\rho) = \sqrt{N_{RN}^2 + N_{PC}^2 + N_{DC}^2}$$

This can then be converted into the relative uncertainty of the flux (in units of W/m^2/μm/sr) by:

$$\Delta F = R * \frac{N}{t_{exp} * g}$$

where R is the radiometric calibration constant for the filter used (Klaasen et al. 2013), t_{exp} the exposure time (seconds), and g the gain (28.5 DN/e).

2. Surface brightness profiles: the noise (in units of electrons) in the surface brightness at a distance r from the nucleus is calculated by the standard deviation of the surface brightness $S(r)$ in a one-pixel-wide annulus with radius r.

3. Flux in large apertures: The flux in the large apertures is calculated by integrating over the derived surface brightness profiles. We empirically determined an upper limit to the noise in this flux by calculating the integrals of the surface brightness profile, plus and minus the uncertainty in the surface brightness. Half of the difference between these two integrals is then the uncertainty in the flux.

4 Known Constraints

1. Our photometric methods do not include a background subtraction, see Sec. 3.6.
2. Images were not corrected for correlated noise (Klaasen et al. 2013).

5 Data Tables

We saved the results in 6 flat ASCII tables:

1. Azimuthally averaged surface brightness profiles
2. Error of surface brightness profiles
3. Small aperture photometry
4. Error of small aperture photometry
5. Large aperture photometry derived from profiles
6. Error of large aperture photometry

The results are stored in separate files using an identical format, where every row contains the results for one image. For all 6 files, results are given for aperture radii/radial distances of [0, 1, 2, 3, 4, 5, 6, 7, 8, 9, 10, 12, 14, 16, 18, 20, 25, 30, 35, 40, 45, 50, 55, 60, 80, 100, 120, 140, 160, 180, 200, 220, 240, 248] pixels. A value of -99 indicates photometry was not computed for the given aperture (i.e. aperture photometry with r < 3 pixels or r > 20 pixels, and azimuthal profile integrals with r<10 pixels or r larger than the size of the detector) are labeled '-99' (we chose to include those so that all tables in this dataset have the same format). The tables all contain further information including the observing date, exposure time, the filter used, and the distances to the comet and Sun. The different columns contain the following information:

Column	**Parameter**	**Unit**	**Comments**
0	File name	N/A	
1	Julian Date	UTC	Midpoint of observation
2	DOY	UTC	Rounded to lowest integer
3	MRI Filter		
4	X-position comet	Pixels	
5	Y-position comet	Pixels	
6	Exposure time	Seconds	
7	Frame size	Pixels	
8	X-distance comet	Pixels	Distance of comet centroid from horizontal boundary between CCD quadrants
9	Y-distance comet	Pixels	Distance of comet centroid from vertical boundary between CCD quadrants
10	Quality Flag		Data with QF > 2 is excluded here. 0 = good; 1 = star nearby; 2 = cosmic ray nearby
11	Heliocentric distance	AU	
12	Spacecraft distance	Km	Distance to center of comet
13	Phase angle	degrees	Sun-comet-spacecraft angle
14	Solar elongation	degrees	Sun-spacecraft-comet angle
15 – 49	Flux	$W/m^2/\mu m$	Files 3 – 6. A value of -99 indicates photometry was not computed for the given aperture.
15 - 49	Surface Brightness	$W/m^2/\mu m/sr$	Files 1 – 2. A value of -99 indicates photometry was not computed for the given aperture.

6 Differences with respect to Photometry V1

- Significant update of photometry documentation
- Added surface brightness profile table
- Photometry with different filters is now given in one file rather than in separate files for ease of comparison
- Error calculation updated (see Sec. 3)
- Added exposure time to data tables
- Added radius of 0 pixels to results so that table format is the same for all data files (profiles, photometry, errors)
- Marked photometry values at apertures in radii not recommended for given photometry method as '-99'
- Marked photometry in apertures larger than chip size as '-99'

7 References

Belton, M.J.S., K.J, Meech, Karen, S. Chesley, et al., 2011, *'Stardust-NExT, Deep Impact, and the accelerating spin of 9P/Tempel 1'*, Icarus, Volume 213, Issue 1, p. 345-368, doi:10.1016/j.icarus.2011.01.006.

Hampton, D.L., J.W. Baer, M.A. Huisjen, et al., 2005, An Overview of the Instrument Suite for the Deep Impact Mission, Space Science Reviews, 117, 43-93, doi:10.1007/s11214-005-3390-8.

Klaasen, K.P., M.F. A'Hearn, M. Baca, et al., 2008, Deep Impact Instrument Calibration, Rev. Sci. Instrum., 79, 091301, doi:10.1063/1.2972112.

Klaasen, K.P., S. Besse, D. Bodewits, et al., 2013, EPOXI Instrument Calibration, Icarus 225, p643.

McLaughlin, S.A., B. Carcich, S.E. Sackett, and K.P. Klaasen, 2012, Epoxi 103P/HARTLEY2 Encounter - MRI Calibrated Images V1.0, NASA Planetary Data System, DIF-C-MRI-3/4-EPOXI-HARTLEY2-V1.0, http://pdssbn.astro.umd.edu/holdings/dif-c-hriv-3_4-epoxi-hartley2-v1.0.